Am J Physiol Cell Physiol 285: C222–C235, 2003.
First published March 26, 2003; 10.1152/ajpcell.00006.2003.

Caveolin-1-deficient mice show insulin resistance and defective insulin receptor protein expression in adipose tissue

Alex W. Cohen,[1,2] Babak Razani,[1,2] Xiao Bo Wang,[1,2] Terry P. Combs,[3] Terence M. Williams,[1,2] Philipp E. Scherer,[3] and Michael P. Lisanti[1,2]

[1]*Department of Molecular Pharmacology, Albert Einstein College of Medicine, Bronx;*
[2]*Division of Hormone-dependent Tumor Biology, The Albert Einstein Cancer Center, Bronx;*
and [3]*Department of Cell Biology, Albert Einstein College of Medicine, Bronx, New York 10461*

Submitted 7 January 2003; accepted in final form 19 March 2003

Cohen, Alex W., Babak Razani, Xiao Bo Wang, Terry P. Combs, Terence M. Williams, Philipp E. Scherer, and Michael P. Lisanti. Caveolin-1-deficient mice show insulin resistance and defective insulin receptor protein expression in adipose tissue. *Am J Physiol Cell Physiol* 285: C222–C235, 2003. First published March 26, 2003; 10.1152/ajpcell.00006.2003.—Several lines of evidence suggest that a functional relationship exists between caveolin-1 and insulin signaling. However, it remains unknown whether caveolin-1 is normally required for proper insulin receptor signaling in vivo. To address this issue, we examined the status of insulin receptor signaling in caveolin-1 (−/−)-deficient (Cav-1 null) mice. Here, we show that Cav-1 null mice placed on a high-fat diet for 9 mo develop postprandial hyperinsulinemia. An insulin tolerance test (ITT) revealed that young Cav-1 null mice on a normal chow diet are significantly unresponsive to insulin, compared with their wild-type counterparts. This insulin resistance is due to a primary defect in adipose tissue, as evidenced by drastically reduced insulin receptor protein levels (>90%), without any changes in insulin receptor mRNA levels. These data suggest that caveolin-1 acts as a molecular chaperone that is necessary for the proper stabilization of the insulin receptor in adipocytes in vivo. In support of this notion, we demonstrate that recombinant expression of caveolin-1 in Cav-1 null mouse embryo fibroblasts rescues insulin receptor protein expression. These data provide evidence that the lean body phenotype observed in the Cav-1 knockout mice is due, at least in part, to a defect in insulin-regulated lipogenesis.

caveolae; caveolin; insulin signaling; protein stabilization; knockout mice

CAVEOLAE are small, morphologically distinct, flask-shaped organelles most commonly found in terminally differentiated cells. They were first identified in the early 1950s on the surface of epithelial cells, where they were suggested to function as endocytic vesicles (23, 48). Further research expanded the proposed role of caveolae to include other functions, such as transcytosis and a concentrating point for certain membrane-bound proteins.

In 1992, an explosion in the field occurred with the discovery of caveolin (now called caveolin-1) as a protein marker and principal component of caveolae (32). This allowed for the development of purification techniques that permitted the biochemical study of caveolae microdomains.

In subsequent years, two other caveolins were discovered, now termed caveolin-2 and caveolin-3 (37, 44). The tissue distributions of the various caveolins have been well studied, and it is now widely accepted that caveolin-1 is found most abundantly in the adipocyte, endothelial, and epithelial cells, whereas caveolin-3 is found in skeletal and cardiac myocytes. The distribution of caveolin-2 most closely follows that of caveolin-1, where it forms functional heterooligomers with caveolin-1 of about 14–16 individual subunits (36, 44).

Caveolae are now known to be much more than the endocytic vesicles they were once thought to be. Many new discoveries have led to the proposal of the "caveolae signaling hypothesis," which attributes the regulation of numerous signaling molecules to a direct relationship with the caveolins (22). Regarding caveolin-1, the majority of these relationships are those of inhibition, as is the case with molecules such as endothelial nitric oxide synthase, Src family tyrosine kinases, EGF receptor, G proteins, and PKA (30, 45). Recently, however, caveolin-1 has also been shown to activate certain signaling molecules, i.e., the insulin receptor (21, 45).

With the development of caveolin-1-deficient (Cav-1 null) mice, a new area of research has emerged, because all of the proposed functions of caveolin-1 can now be tested in vivo. The first publications regarding this animal (6, 27, 28, 31) describe a viable and fertile mouse with a hyperproliferative lung phenotype, exercise intolerance, and, more recently, abnormalities in lipid homeostasis.

In our report on this subject (31), we showed that Cav-1 null mice are resistant to diet-induced obesity and demonstrate significant white adipose tissue atrophy with age. Although the pathogenesis of these findings was not elucidated, we also showed that Cav-1 null mice are hypertriglyceridemic (in both the fasted and postprandial state) and have elevated serum levels of free fatty acids in the postprandial state. In addition,

Address for reprint requests and other correspondence: M. P. Lisanti, Dept. of Molecular Pharmacology, Albert Einstein College of Medicine, 1300 Morris Park Ave., Bronx, NY 10461 (E-mail: lisanti@aecom.yu.edu).

The costs of publication of this article were defrayed in part by the payment of page charges. The article must therefore be hereby marked "*advertisement*" in accordance with 18 U.S.C. Section 1734 solely to indicate this fact.

these mice are unable to clear a triglyceride load, as evidenced by the kinetic buildup of triglyceride-rich chylomicrons/very low-density lipoproteins in the blood after administration of a fat bolus. We also found that two adipokines, Acrp30 and leptin, a lack of which has been associated with insulin resistance, are significantly reduced in their plasma concentrations. These changes occurred without any noticeable differences in other plasma metabolites, such as glucose, insulin, or cholesterol.

Here, we elucidate the molecular mechanism underlying these adipocyte-based phenotypes in Cav-1 null mice. One of the major functions of insulin signaling in the adipocyte is to activate lipogenesis and inhibit lipolysis. Previous in vitro studies have shown that caveolin-1 can interact with the insulin receptor and enhance insulin-mediated phosphorylation of IRS-1 (21, 49). Thus, if these findings are indeed physiologically relevant, it would be predicted that loss of caveolin-1 should dampen insulin receptor signaling, leading to unregulated lipolysis and a reduction of lipogenic signals. In support of this notion, we show that Cav-1 null mice develop postprandial hyperinsulinemia on a high-fat diet and demonstrate insulin insensitivity. Furthermore, we show that these defects are due to a primary defect in insulin signaling in the adipocyte at the level of the insulin receptor itself.

MATERIAL AND METHODS

Materials. The cDNAs for wild-type (WT) full-length caveolin-1 (1–178) and caveolin-1 (Δ61–100) were subcloned into the cytomegalovirus-based vector pCB7 as previously described (36, 38). The insulin receptor full-length cDNA was the gift of Dr. Jonathan Backer (Albert Einstein College of Medicine). Antibodies and their sources were as follows: anti-caveolin-1 IgG (N-20), anti-insulin receptor (IR)-β (C-19), and anti-insulin-like growth factor (IGF)-1 receptor-β (C-20; PAb), all from Santa Cruz Biotechnology (Santa Cruz, CA); anti-phospho-tyrosine clone 4G10 (MAb), anti-phospho-PKB/Akt (S473; PAb), anti-phospho-glycogen synthase kinase (GSK)-3 (Y216; MAb), and anti-phosphatidylinositol (PI) 3-kinase (PAb), all from UBI (Haupauge, NY); anti-β-tubulin (MAb) and anti-β-actin (MAb) from Sigma (St. Louis, MO); anti-caveolin-2 (MAb), anti-GSK-3β (MAb), anti-protein phosphatase-2A (PP2A) catalytic α (MAb), and anti-PKB/Akt (PAb), all from BD Transduction Laboratories (Palo Alto, CA); and the insulin-responsive glucose transporter (GLUT-4; MAb) from Genzyme (Cambridge, MA). Recombinant human insulin was purchased from Novo Nordisk (Princeton, NJ). A variety of other reagents were of the highest purity grade and were obtained from the usual commercial sources.

Animal studies. All animals were housed and maintained in a barrier facility at the Institute for Animal Studies, Albert Einstein College of Medicine. Cav-1 (−/−) null mice, Cav-2 (−/−) null mice, and the corresponding WT cohorts were generated and maintained by us, as previously described (28, 31).

High-fat diet study; insulin and glucose measurements. WT and Cav-1 null mice were placed at weaning (3 wk of age) on either a high-fat diet (59% of calories derived from fat; D12492, Research Diets) or a normal chow diet (10% of calories derived from fat; D12450B, Research Diets). At 9 mo, fasting and postprandial plasma insulin levels were measured by radioimmunoassay and fasting serum glucose levels were measured colorimetrically, as we previously described (27).

Insulin tolerance test (ITT). Weight-matched 20-wk-old mice that had been fed a normal chow diet were given an intraperitoneal injection of 0.75 U/kg insulin. Fasted serum glucose levels were then measured at all time points colorimetrically. It is important to note that WT and Cav-1 null mice do not display any statistically significant weight differences at this age (27), and thus the same dose of insulin was given to each mouse.

Muscle triglyceride analysis. Muscle triglycerides were extracted according to the methods of Bligh and Dyer, as described by Iverson et al. (11). Briefly, hindlimb muscle tissue was removed from each mouse (WT, $n = 7$; Cav-1 null, $n = 7$) and promptly frozen in liquid N_2. About 400 mg of tissue were homogenized in 4 ml of extraction buffer (20 mM Tris, pH 7.3, 1 mM EDTA, and 1 mM β-mercaptoethanol). This extract (800 μl) was placed in a glass tube, and 1 ml of chloroform and 2 ml of methanol were added, mixed, and allowed to stand for 30 min. Next, 1 ml of water and 1 ml of chloroform were added, and the samples were mixed and centrifuged for 20 min at 3,000 rpm at 10°C. The upper aqueous layer was discarded, and the lower phase was evaporated under N_2. The sample was redissolved in 250 μl of isopropanol, and true triglycerides were measured using GPO-Trinder (Sigma), according to the manufacturer's instructions.

Immunofluorescence. Mouse embryo fibroblasts (MEFs) were grown on glass coverslips, fixed in 2% paraformaldehyde, and permeabilized in 0.1% Triton X-100. Cells were then immunostained with monoclonal anti-caveolin-1 (cl 2234) and polyclonal anti-insulin receptor-β antibodies. Bound primary antibodies were visualized with a fluorescein-conjugated anti-mouse antibody and a rhodamine-conjugated anti-rabbit antibody (Jackson ImmunoResearch). As expected, omission of the primary antibodies prevented immunostaining.

Immunoblot analysis. Mice were killed, and fat, liver, and muscle samples were harvested and immediately frozen in liquid N_2 (WT, $n \geq 7$; Cav-1 null, $n \geq 7$). Approximately 100 mg of a given tissue sample were then homogenized in lysis buffer [50 mM Tris, pH 8.0, 150 mM NaCl, 50 mM NaF, 30 mM sodium pyrophosphate, 2 nM sodium orthovanadate, 0.1 μg/ml okadaic acid, 40 nM bpVphen, 1% Igepal (formerly NP-40), and 0.5% deoxycholic acid] containing protease inhibitors (Boehringer Mannheim). Tissue lysates were then centrifuged at 12,000 *g* for 10 min to remove insoluble debris. Protein concentrations were analyzed using the BCA reagent (Pierce), and the volume required for 40 μg of protein was determined. Samples were then separated by SDS-PAGE and transferred to nitrocellulose. The nitrocellulose membranes were stained with Ponceau S (to visualize protein bands), followed by immunoblot analysis. All subsequent wash buffers contained 10 mM Tris, pH 8.0, 150 mM NaCl, and 0.05% Tween 20, which were supplemented with 1% bovine serum albumin (BSA) and 2% nonfat dry milk (Carnation) for the blocking solution and 1% BSA for the antibody diluent. Primary antibodies were used at a 1:500 dilution. Horseradish peroxidase-conjugated secondary antibodies (1:5,000 dilution; Pierce) were used to visualize bound primary antibodies with the Supersignal chemiluminescence substrate (Pierce).

Northern blot analysis. Mice were killed, and the perigonadal fat pad was removed and frozen in liquid N_2. Total RNA was extracted from 150 mg of tissue from each sample using the Trizol reagent protocol (GIBCO). Total RNA (20 μg)

for each sample was separated by using a 1.2% agarose gel under RNase-free conditions and transferred to a Hybond-XL nylon membrane (Amersham). The filters were hybridized using the ExpressHyb solution (Clontech). An insulin receptor probe was generated by PCR amplification of a 1.5-kb fragment of the insulin receptor cDNA coding sequence by using custom-synthesized primers (5′-ATGAATTCCAGCAACTTGCTGTGC-3′) corresponding to the first 24 bases and (5′-CTGGTTGCAAGCCTGCAGCTC-3′) corresponding to 21 bases at the 1.5-kb point along the insulin receptor cDNA. This PCR product was then gel purified, radiolabeled, and hybridized to the nylon membrane.

Cell culture. Human embryonic kidney (HEK)-293 cells and MEFs (WT and Cav-1 knockout) were grown in DMEM supplemented with glutamine, antibiotics (penicillin and streptomycin), and 10% fetal calf serum.

Transient transfections. HEK-293 cells and Cav-1 knockout MEFs were transiently transfected with the caveolin-1 cDNA (pCB7-Cav-1) or the caveolin-1 Δ61–100 mutant [pCB7-Cav-1 (Δ61–100)] using either the standard calcium phosphate protocol (for HEK-293) or Lipofectamine Plus reagent [for MEFs; according to the manufacturer's instructions (Invitrogen)]. Thirty-six hours posttransfection, cells were collected into lysis buffer (10 mM Tris, pH 7.5, 50 mM NaCl, 1% Triton X-100, and 60 mM octyl glucoside) containing protease inhibitors (Boehringer Mannheim) and subjected to either SDS-PAGE or Western analysis. Alternatively, cells were examined by immunofluorescence microscopy.

Rescue of insulin receptor levels in Cav-1-deficient MEFs. MEFs were treated with either vehicle alone (Me_2SO) or the proteasomal inhibitor MG-132 (1 μM; Sigma) for the time points indicated. Cells were then lysed and subjected to immunoblot analysis.

RESULTS

Cav-1 null mice develop postprandial hyperinsulinemia on a high-fat diet. In our previous study (31), we found that Cav-1 null mice do not have abnormalities in insulin or glucose levels on a standard chow diet; however, they do demonstrate significant increases in serum triglycerides and free fatty acids, as well as adipose tissue degeneration. One possible explanation for this is that a lack of caveolin-1 leads to unregulated lipolysis and diminished lipogenesis. Previous in vitro studies have shown that caveolin-1 can interact with the insulin receptor and enhance insulin-mediated phosphorylation of IRS-1 (21, 49). Thus, if these findings are indeed physiologically relevant, it would be predicted that loss of caveolin-1 should dampen insulin receptor signaling, leading to unregulated lipolysis and a reduction of lipogenic signals. This would explain the lean body phenotype of Cav-1 null mice that are unable to clear a triglyceride load and fail to suppress free fatty acid levels postprandially.

We did not observe any insulin resistance in mice fed a normal diet, so we chose to mimic a factor that helps to produce this condition in the human population, namely, a high-fat diet. We therefore placed male and female cohorts of WT and knockout mice at weaning (3 wk of age) on either a high-fat diet (59% of calories from fat) or a normal chow diet (10% of calories from fat). At 9 mo of age, fasting and postprandial plasma insulin levels were measured by radioimmunoassay.

Figure 1 shows that all mice exhibited the expected rise in insulin levels in the postprandial state. However, the Cav-1 null mice that were fed a high-fat diet demonstrated statistically significant postprandial hyperinsulinemia compared with WT mice fed the same diet. Importantly, Cav-1 null mice that were fed a normal chow diet did not show any hyperinsulinemia, suggesting that caveolin-1 plays a role in diet-induced insulin resistance. In addition, no statistically significant differences in fasting serum glucose concentrations were observed between WT and Cav-1 null mice on a high-fat diet (females: WT, 126.7 ± 14.4 mg/dl; Cav-1 null, 129.8 ± 17.7 mg/dl; males: WT, 122.8 ± 7.1 mg/dl; Cav-1 null, 128.2 ± 11.0 mg/dl; $n \geq 6$ mice for each experimental group). It is important to note that all the other studies detailed below were performed on young mice fed a normal chow diet.

Cav-1 null mice show a blunted response to insulin, as assessed by ITT. Because hyperinsulinemia is generally a result of underlying insulin resistance, we next sought to determine whether Cav-1 knockout mice show any changes in insulin responsiveness. Weight-matched 20-wk-old Cav-1 null and WT mice that had been fed a normal chow diet were given an intraperitoneal injection of insulin (0.75 U/kg). Fasted serum glucose levels were then measured at all time points for all mice colorimetrically.

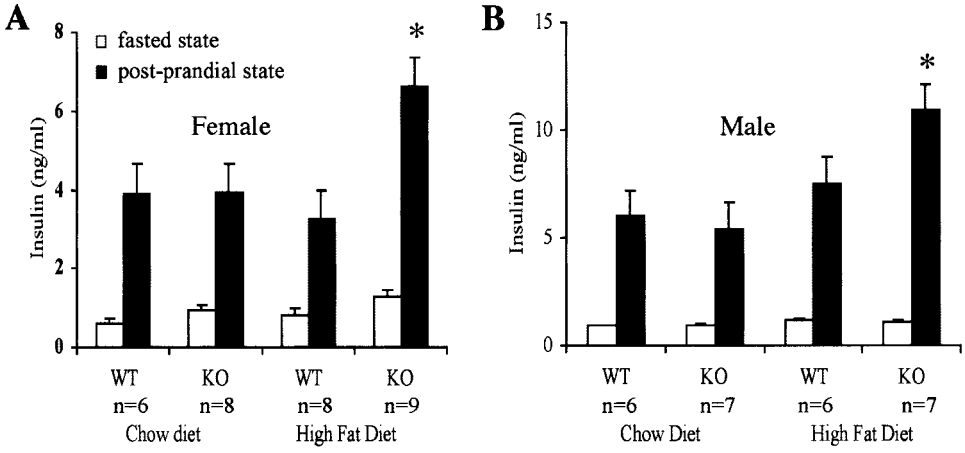

Fig. 1. Cav-1 null mice placed on a high-fat diet develop postprandial hyperinsulinemia compared with their wild type (WT) counterparts. Age-matched cohorts of WT and Cav-1 knockout (KO) mice were placed at weaning (3 wk of age) on a standard chow diet (10% of calories from fat) or a high-fat diet (59% of calories from fat). At 9 mo of age, fasting blood samples were collected at 7:00 AM (12 h after removal of food) and postprandial blood samples were collected at 12:00 AM (after 3 h of feeding in the dark). Plasma insulin levels were measured by radioimmunoassay. *A*: female; *B*: male. Values are means ± SE; n = no. of mice. *Significant difference between WT and KO mice ($P < 0.05$).

Figure 2 shows the expected decline in glucose levels after the administration of insulin (due to glucose uptake in peripheral tissues). Baseline glucose levels for both cohorts of mice are indistinguishable. However, most importantly, Cav-1 null mice showed a markedly blunted decline in glucose levels upon insulin injection, indicative of peripheral insulin resistance.

Cav-1 null mice do not demonstrate fat deposition at ectopic sites. Obesity is associated with the development of insulin resistance and type II diabetes in humans and rodents. Although the cause of this association is not known, many have suggested that fat deposition outside of the adipocyte is to blame, the so-called "lipotoxicity theory" (8). This theory states that when lipid accumulates in insulin-sensitive tissues other than fat, an inhibition of insulin action results. Therefore, it is possible that ectopic fatty deposits are the cause of the observed postprandial hyperinsulinemia in Cav-1 null mice.

To this end, we used a modified Bligh and Dyer extraction protocol to measure the triglyceride content of hindlimb muscle in both WT and Cav-1 null mice. Muscle samples were removed from each mouse, weighed, and homogenized. A portion of this homogenate was then subjected to chloroform-methanol phase separation. After evaporation of the chloroform layer, total and free triglyceride contents were measured colorimetrically, from which the true triglyceride content was calculated. Our analysis shows that there is no significant difference between the lipid content of skeletal muscle obtained from Cav-1 null or WT mice (WT, 17.48 ± 4.14 μg/mg tissue; Cav-1 null, 17.84 ± 5.35 μg/mg tissue). Thus it appears that "lipotoxicity" does not play a role in the postprandial hyperinsulinemia observed in Cav-1 null mice.

Cav-1 null mice have a primary defect in insulin signaling in the adipocyte. Because it appears that insulin resistance in Cav-1 null mice is not due to ectopic fat deposits, we next turned our attention to the more intriguing culprit, the adipocyte. The observed postprandial hyperinsulinemia and insulin resistance are consistent with findings demonstrating a role for caveolin-1 in enhancing insulin signaling, so we sought to determine whether this phenotype is a result of a primary defect in the Cav-1 null adipocyte.

Cav-1 null and WT mice that had been fed a normal chow diet were intraperitoneally injected with insulin (1 U/kg) for 7.5 min and then killed by CO_2 asphyxiation. Perigonadal fat pads were then immediately removed and frozen in liquid N_2. These samples were then homogenized in lysis buffer, and equal amounts of protein were subjected to Western blot analysis. Because the insulin receptor is composed of two extracellular α-subunits and two transmembrane β-subunits that are normally tyrosine phosphorylated in response to insulin binding, we chose to look at the phosphorylation state of the β-subunit as a marker for insulin receptor activity. Interestingly, we found a dramatic reduction in insulin receptor-β (IR-β) tyrosine phosphorylation/activation in the Cav-1 knockout mouse (Fig. 3*A*). However, upon further analysis, we deduced that this reduction in IR-β tyrosine phosphorylation is due to the downregulation of the insulin receptor protein itself in Cav-1 null adipose tissue (Fig. 3*A*). Thus Cav-1 null mice have an insulin receptor deficiency (>90% reduced) in adipose tissue.

To determine whether this reduction in IR-β protein levels is selective for adipose tissue, we next examined the status of IR-β levels in other insulin-responsive tissues that do not contain an abundance of caveolin-1,

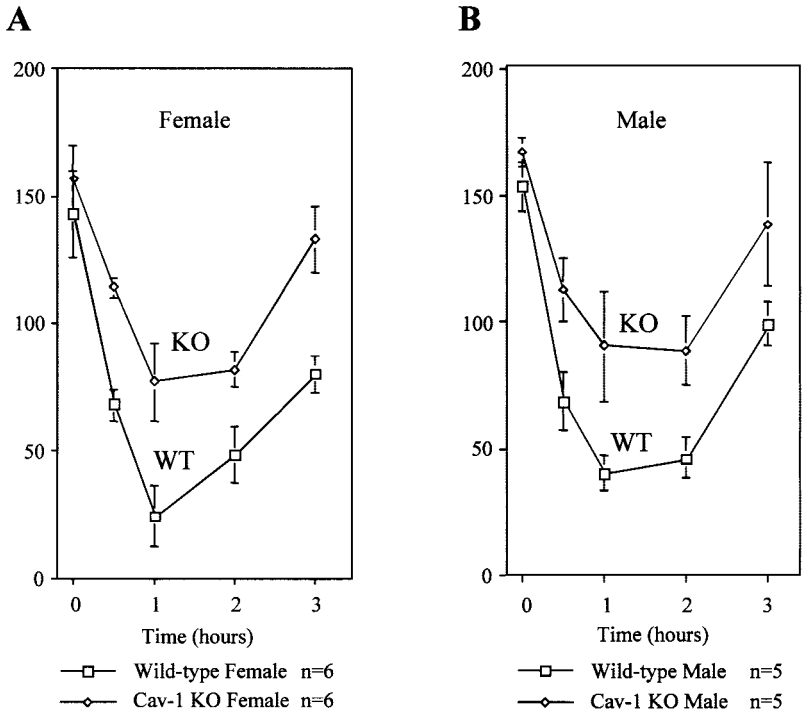

Fig. 2. Cav-1-null mice display insulin resistance, as assessed using an insulin tolerance test (ITT). Insulin (0.75 U/kg) was administered to a cohort of weight-matched 5-mo-old WT and Cav-1 KO mice by intraperitoneal injection. Blood samples were obtained from the tail vein at baseline and at 30 min, 1 h, 2 h, and 3 h. Glucose was measured calorimetrically for all mice at all time points. *A*: female; *B*: male. The results are displayed as means ± SE for each cohort. WT and Cav-1 KO mice do not display any statistically significant weight differences at this age (27), and thus the same dose of insulin was given to each mouse.

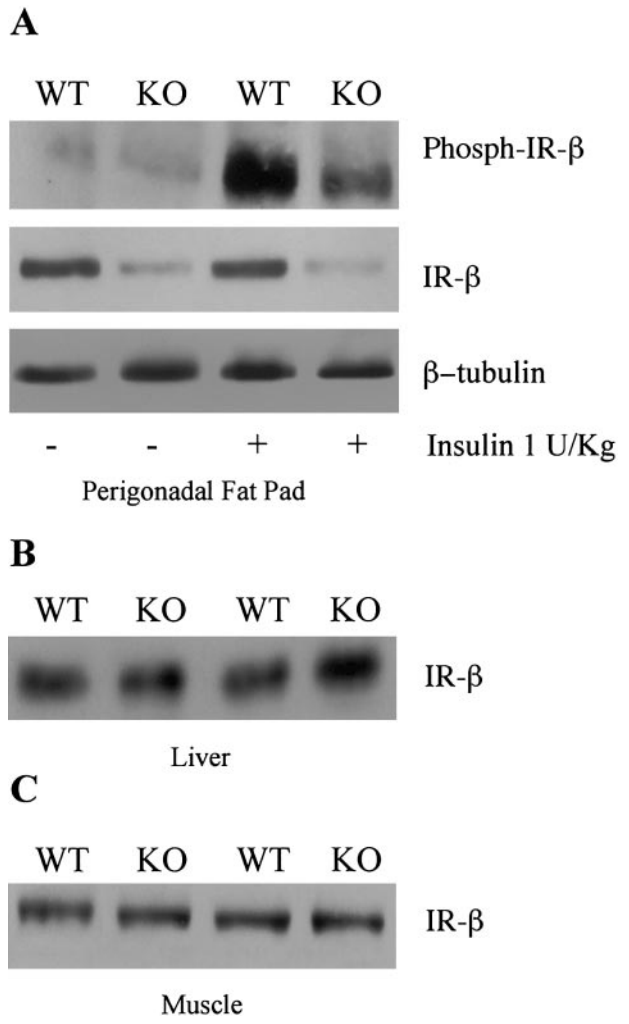

Fig. 3. Cav-1 null mice show blunted insulin receptor (IR)-β activation and decreased protein expression levels of IR-β selectively in adipose tissue. Insulin (1.0 U/kg) was administered to a cohort of WT and Cav-1 KO mice by intraperitoneal injection. The mice were killed by CO_2 asphyxiation at 7.5 min postinjection. The perigonadal fat pads were then removed and homogenized in lysis buffer. Western blot analysis of the lysates shows that insulin treatment failed to stimulate the tyrosine phosphorylation of the IR-β subunit in Cav-1 KO mice to the same extent as in WT mice (*A*). Immunoblotting for total IR-β protein shows a dramatic reduction in Cav-1 KO mice compared with WT controls. β-Tubulin is shown as a control for equal protein loading. Also, the IR-β content of liver (*B*) and skeletal muscle (*C*) remained unaffected in Cav-1 KO mice.

i.e., skeletal muscle and liver. As might be predicted, neither liver nor skeletal muscle tissue samples from Cav-1 null mice showed any changes in IR-β protein levels (Fig. 3, *B* and *C*). These findings provide the first in vivo evidence for an interaction between caveolin-1 and the insulin receptor, because it appears that caveolin-1 is necessary for insulin receptor stabilization in adipocytes.

Cav-2 null mice do not show any changes in insulin receptor levels. As we previously reported, caveolin-1 deficiency in mice leads to an ~95% reduction in caveolin-2 protein levels, because caveolin-1 protein expression is required to stabilize the caveolin-2 protein product (28, 29). Therefore, Cav-1 null mice are essentially deficient in both caveolin-1 and caveolin-2.

To determine whether downregulation of insulin receptor protein levels in Cav-1 null mice is due to the loss of caveolin-1 or caveolin-2, we also examined insulin receptor levels in adipose tissue samples derived from Cav-2 null mice. As shown in Fig. 4, the protein levels of insulin receptor-β were not altered in Cav-2 null mice. Therefore, we can conclude that the disruption of the insulin receptor is dependent on the status of caveolin-1 but not caveolin-2. This is consistent with our previous observations that Cav-2 null mice have normal adipose tissue and clearly do not share the abnormal adipose tissue phenotype observed in Cav-1 null mice (31).

Insulin receptor mRNA levels remain unchanged in Cav-1 null adipose tissue. To determine whether the change in insulin receptor protein expression is due to transcriptional downregulation in Cav-1 null mice, we next used Northern blot analysis to quantify the amount of insulin receptor mRNA in Cav-1 null adipose tissue. Total RNA was isolated from perigonadal fat pads using the Trizol reagent, separated on an agarose gel, and then transferred to a Hybond-XL nylon membrane. Primers were then used to construct a 1.5-kb probe by PCR from a plasmid containing the entire insulin receptor cDNA. The probe was gel purified, quantified, labeled with [^{32}P]dCTP, and hybridized to the nylon membrane.

Our results show that there is no difference between the quantity of insulin receptor mRNA in Cav-1 null mice compared with WT mice. The 18S and 28S rRNA are shown as a control for equal loading (Fig. 5).

Insulin-like growth factor-1 receptor protein levels remain unchanged in Cav-1 null adipose tissue. The insulin receptor is one of a family of receptor tyrosine kinases that includes the IGF-1 receptor (IGF-1R). Both receptors are composed of structurally similar subunits, termed α and β, that are known to form functional hybrid dimers in cells that have both receptors. Furthermore, a certain degree of overlap is known to exist between these two receptors for their native ligands, insulin and the IGFs (20, 33).

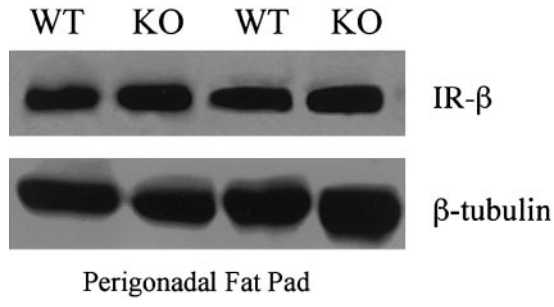

Fig. 4. Protein expression levels of the IR-β are not altered in Cav-2 null mice. Perigonadal fat pads were harvested from Cav-2 KO mice and homogenized in lysis buffer. Lysates were subjected to SDS-PAGE and immunoblotted with anti-IR-β. *Top*: there is no observable difference in the amount of insulin receptor protein between Cav-2 KO mice and their WT cohorts. *Bottom*: β-tubulin was used as a control for equal protein loading.

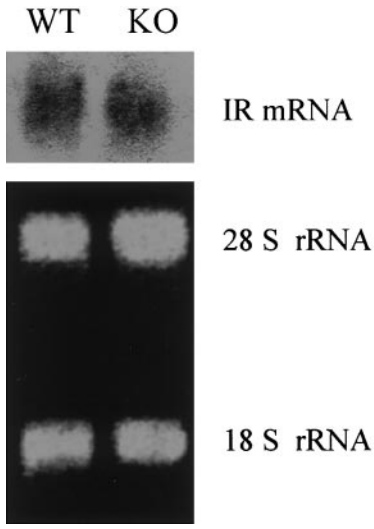

Fig. 5. Levels of the insulin receptor mRNA are not altered in Cav-1 null mice. Perigonadal fat pads harvested from WT and Cav-1 KO mice were promptly frozen in liquid nitrogen. Total RNA was then extracted for Northern analysis. Note that the levels of the insulin receptor mRNA were not altered in Cav-1 KO mice. The abundance of 18S and 28S rRNA are shown as a control for equal loading.

Because the Cav-1 knockout mice are able to maintain euglycemia while the level of insulin receptor protein is drastically decreased, we sought to determine the role of the IGF-1R in glucose metabolism in these mice. As described above, we removed perigonadal fat pads from killed mice, homogenized them in lysis buffer, and subjected these lysates to SDS-PAGE. Immunoblotting of nitrocellulose membranes with antibodies specific for IGF-1Rβ showed that there is no difference between WT and Cav-1 null mice in this regard (Fig. 6). Thus there is no compensatory upregulation of IGF-1R in Cav-1 knockout mice.

GLUT-4 and PKB/Akt are upregulated in Cav-1 null adipose tissue. Because the signals generated by insulin and the insulin receptor itself are drastically diminished in Cav-1 null adipose tissue, we next examined the levels of several proteins downstream of the insulin receptor in the insulin signaling cascade to detect a possible compensatory upregulation of these signaling molecules.

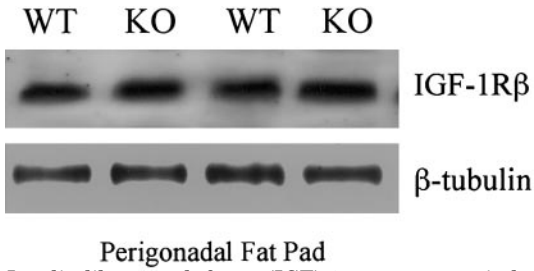

Fig. 6. Insulin-like growth factor (IGF)-1 receptor protein levels are normal in Cav-1 null mice. Perigonadal fat pads harvested from WT and Cav-1 KO mice were subjected to Western blot analysis for IGF-1 receptor-β (IGF-1Rβ) protein expression. *Top*: IGF-1Rβ levels remained unaffected in Cav-1 KO mice. *Bottom*: β-tubulin was used as a control for equal protein loading.

Perigonadal fat pads were homogenized in lysis buffer and subjected to Western analysis. As shown in Fig. 7*A*, we found that the levels of GLUT-4 were dramatically increased in Cav-1 null mice, possibly as a response to the postprandial hyperinsulinemia. Other groups have previously reported that GLUT-4 levels are elevated in response to hyperinsulinemia (3, 5). Furthermore, a recent report indicates that, in 3T3L1 adipocytes, disruption of caveolae with cholesterol chelating agents results in an insulin-independent increase in plasma membrane GLUT-4 (39).

We also found that PKB/Akt levels were increased (Fig. 7*B*), perhaps in response to reduced insulin sig-

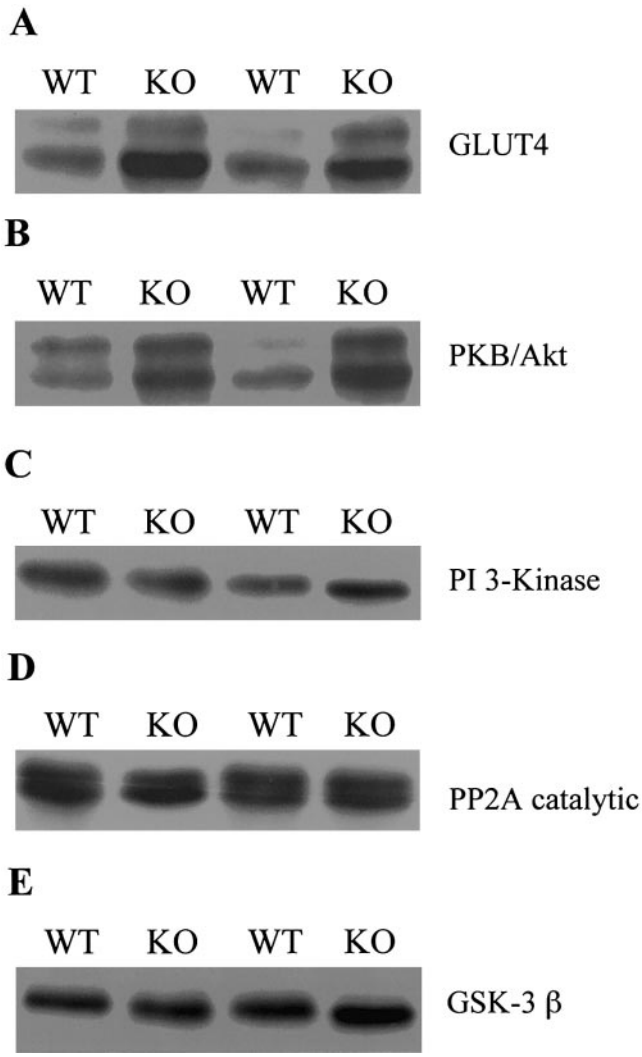

Fig. 7. Cav-1 null mice show increased levels of GLUT-4 and PKB/Akt in adipose tissue. *A*: Western blot analysis of WT and Cav-1 KO perigonadal fat pads revealed increased levels of the insulin-responsive glucose transporter GLUT-4 in Cav-1 KO mice. *B*: Cav-1 KO mice also show higher levels of PKB/Akt, a downstream molecule in the insulin signaling cascade responsible for promoting glycogen synthesis and inducing GLUT-4 translocation to the plasma membrane. However, other downstream targets of insulin stimulation [phosphatidylinositol (PI) 3-kinase, protein phosphatase 2A (PP2A) catalytic subunit, and glycogen synthase kinase (GSK)-3β] do not show any changes in their protein expression levels in Cav-1 KO adipose tissue (*C–E*).

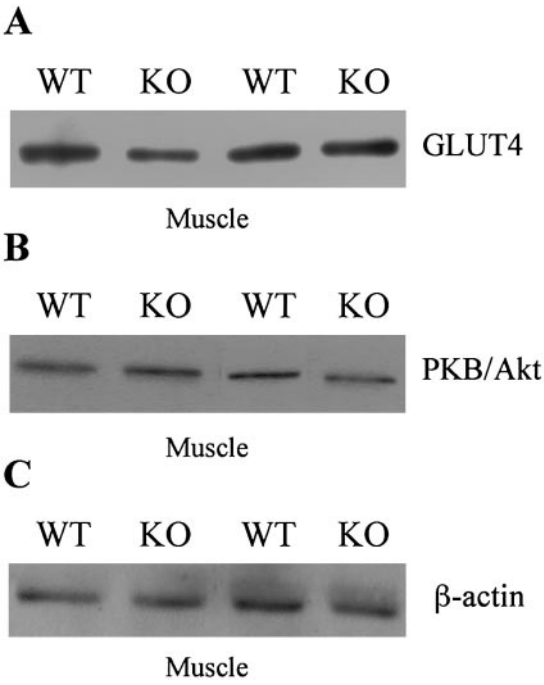

Fig. 8. GLUT-4 and PKB/Akt protein levels are not changed in Cav-1 null skeletal muscle samples. Analysis similar to that in Fig. 7 reveals that the changes in GLUT-4 and PKB/Akt are specific for adipose tissue, because skeletal muscle samples do not exhibit any differences in their expression of either protein (*A* and *B*, respectively). *C*: β-actin was used as a measure of equal protein loading.

naling, because Akt normally functions to induce GLUT-4 translocation to the membrane and promotes glycogen synthesis via inactivation of GSK-3β (19, 46).

However, other proteins in the insulin signaling cascade remained unchanged in their expression levels (Fig. 7, *C–E*). PI 3-kinase, which activates PKB/Akt, GSK-3β, a major target of Akt, and the catalytic domain of PP2A, a phosphatase that inactivates the PI 3-kinase/PKB pathway, remain unchanged in their protein expression levels compared with WT controls.

In addition, the observed increases in GLUT-4 and PKB/Akt expression levels are limited to the adipocyte, because skeletal muscle samples do not show any changes in either GLUT-4 or PKB/Akt protein levels (Fig. 8, *A* and *B*).

Insulin-stimulated phosphorylation is diminished selectively in Cav-1 null adipose tissue. As shown in Fig. 3*A*, using Cav-1 null mice, we demonstrated a ~90% selective reduction in insulin receptor protein levels and a corresponding decrease in insulin-stimulated phosphorylation of this receptor in the adipocyte, whereas insulin receptor protein levels remained unchanged in the liver and muscle. To demonstrate that the liver and muscle tissue of Cav-1 null mice are capable of transmitting insulin signals normally, we again stimulated mice with insulin (7.5 min, 1 U/Kg) and probed these tissues for phosphorylated IR-β. As shown in Fig. 9*A*, liver and muscle tissues showed equivalent IR-β phosphorylation in both WT and Cav-1

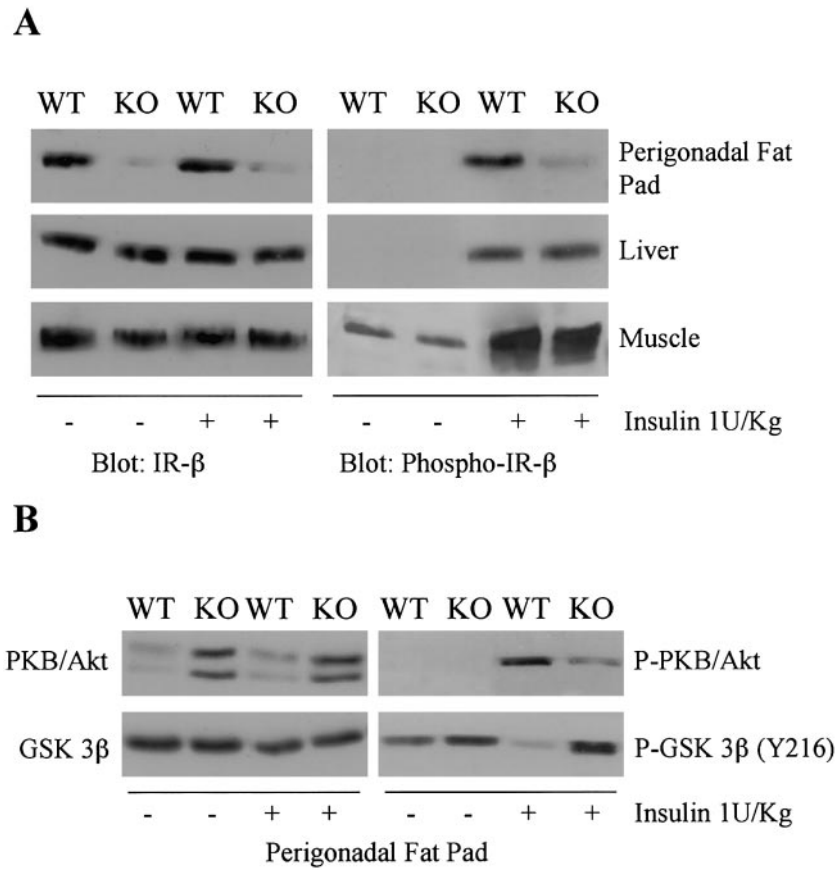

Fig. 9. Cav-1 null adipose tissue selectively fails to properly transduce insulin signals. *A*: as in Fig. 3, mice were given an intraperitoneal injection of insulin. After 7.5 min, the mice were killed, and their insulin-sensitive tissues were harvested for Western blot analysis. Note that, upon insulin stimulation, phospho-IR-β levels increased in the liver and muscle of both WT and Cav-1 KO mice. However, in the perigonadal fat pad of Cav-1 KO mice, total IR-β protein levels were decreased; thus insulin caused minimal phosphorylation of the receptor. *B*: the perigonadal fat pads were also subjected to Western blot analysis with antibodies specific for the phosphorylated states of two insulin-responsive signaling molecules, PKB/Akt and GSK-3β. Note that insulin treatment failed to stimulate PKB/Akt activation in Cav-1 null mice. Similarly, insulin also failed to cause the normal dephosphorylation of GSK-3β on tyrosine 216 (Y216).

null mice, whereas IR-β phosphorylation, along with IR-β itself, were again diminished in the perigonadal fat pad. These results provide strong evidence that reduced insulin signaling occurs selectively in Cav-1 null adipose tissue.

To determine whether the reduced insulin receptor protein and phosphorylation levels have any functional consequence on insulin signaling in the adipocyte, we next examined the activation state of two downstream signaling molecules, PKB/Akt and GSK-3β. PKB/Akt is normally activated by phosphorylation on serine 473 in response to insulin stimulation. In contrast, GSK-3β is controlled by dual phosphorylation. Phosphorylation of tyrosine 216 leads to activation, whereas inactivation occurs *1*) by phosphorylation of serine 9, by PKB/Akt, and *2*) by dephosphorylation of tyrosine 216 (7). Thus GSK-3β is normally dephosphorylated on tyrosine 216 in response to insulin stimulation.

Interestingly, we found that, after insulin treatment, phospho-PKB/Akt levels were greatly reduced in Cav-1 null adipose tissue compared with WT controls (Fig. 9*B*). Furthermore, in Cav-1 null adipose tissue, phospho-GSK-3β (Y216) levels failed to decrease after insulin administration (Fig. 9*B*). These results indicate that the reduced insulin receptor protein levels and decreased activation of the insulin receptor lead to an overall diminishment of downstream insulin signaling events, as predicted.

Recombinant expression of caveolin-1 in Cav-1 null fibroblasts rescues insulin receptor expression. Our in vivo results clearly show that in the absence of caveolin-1, the insulin receptor protein was found in diminished quantity selectively in the adipocyte (see Fig. 3). These results suggest that the insulin receptor is somehow normally stabilized in the presence of caveolin-1.

To further explore the supporting role that caveolin-1 appears to play for the insulin receptor, we next moved to cell culture systems to examine whether recombinant expression of caveolin-1 can rescue or upregulate insulin receptor expression in caveolin-deficient cells. For this purpose, we chose to use two different fibroblastic cell lines, HEK-293 cells, which express extremely low levels of endogenous caveolin-1, and 3T3 fibroblasts derived from WT and Cav-1 null mouse embryos (28, 42).

To determine whether MEFs provide a good model for dissecting the mechanisms underlying our findings in whole animals, we first compared WT and Cav-1 null MEFs for insulin receptor content by Western blot analysis. As shown in Fig. 10*A*, Cav-1 null MEFs contained significantly less IR-β protein compared with WT MEFs, in accordance with our findings using adipose tissue.

We next transiently expressed caveolin-1 in both MEFs and HEK-293 cells. Thirty-six hours posttransfection, the cells were lysed and analyzed via Western blot for caveolin-1 and insulin receptor expression. As shown in Fig. 10, *B* and *C*, we found that transient expression of caveolin-1 dramatically increased the amount of IR-β present in both Cav-1 null 3T3 MEFs and HEK-293T cells.

Virtually identical results were also obtained by immunofluoresence analysis. Cav-1 null 3T3 fibroblasts transfected with the caveolin-1 cDNA showed a marked increase in insulin receptor immunostaining, whereas neighboring untransfected cells revealed very low or undetectable levels of IR-β immunostaining (Fig. 10*D*).

Thus our findings indicate that caveolin-1 has a dramatic effect on insulin receptor protein levels in both fibroblasts and adipocytes. These data are consistent with the well-accepted notion that fibroblasts are adipocyte precursors during the process of adipocyte differentiation.

The insulin receptor is degraded by the proteasomal pathway. To gain insight into the mechanism by which loss of caveolin-1 could lead to a reduction in insulin receptor protein levels, we next focused on the cellular degradative machinery. Specifically, we chose to examine the role of the proteasomal pathway using the well-known inhibitor MG-132 (28). Cav-1 null MEFs were treated with 1 μM MG-132 over a time course of 6 and 12 h and were then assayed for insulin receptor protein levels via Western blot analysis.

Figure 11 demonstrates a dramatic rescue of the IR-β subunit as early as 6 h posttreatment. This finding provides further evidence that caveolin-1 indeed stabilizes the insulin receptor against cellular degradation processes. Caveolin-2 is shown as a positive control because it has previously been shown to be rescued by proteasomal inhibition (28), whereas β-tubulin is shown as a control for equal protein loading.

Recombinant expression of Cav-1 (Δ61–100) in Cav-1 null fibroblasts fails to rescue insulin receptor protein expression. A multitude of studies have given rise to the idea that caveolin-1 interacts with numerous proteins via a cytoplasmic NH_2-terminal domain contained within residues 61–101, termed the oligomerization domain, or a region therein (residues 82–101), termed the scaffolding domain (reviewed in Ref. 22). To further explore the relationship between caveolin-1 and the insulin receptor, we used an oligomerization/scaffolding domain-deficient caveolin-1 construct, Cav-1 (Δ61–100), to determine whether this portion of the protein is necessary for insulin receptor stabilization.

Caveolin-1-deficient MEFs were transiently transfected with either full-length WT Cav-1 (as in Fig. 11) or Cav-1 (Δ61–100). The cells were then lysed and subjected to Western analysis for IR-β levels. As predicted, the Cav-1 (Δ61–100) mutant failed to rescue insulin receptor levels, unlike full-length Cav-1 (Fig. 12*A*). We next used immunofluorescence microscopy to further evaluate our results from immunoblot analysis. Note that the cell transfected with Cav-1 (Δ61–100) (Fig. 12*B*, arrow) shows no change in insulin receptor immunostaining compared with the surrounding untransfected cells (arrowheads). See Fig. 10*D* for comparison with WT Cav-1. Thus the above results are consistent with the notion that the Cav-1 scaffolding domain may play a protective role in stabilizing the insulin receptor, thereby preventing its proteasomal degradation.

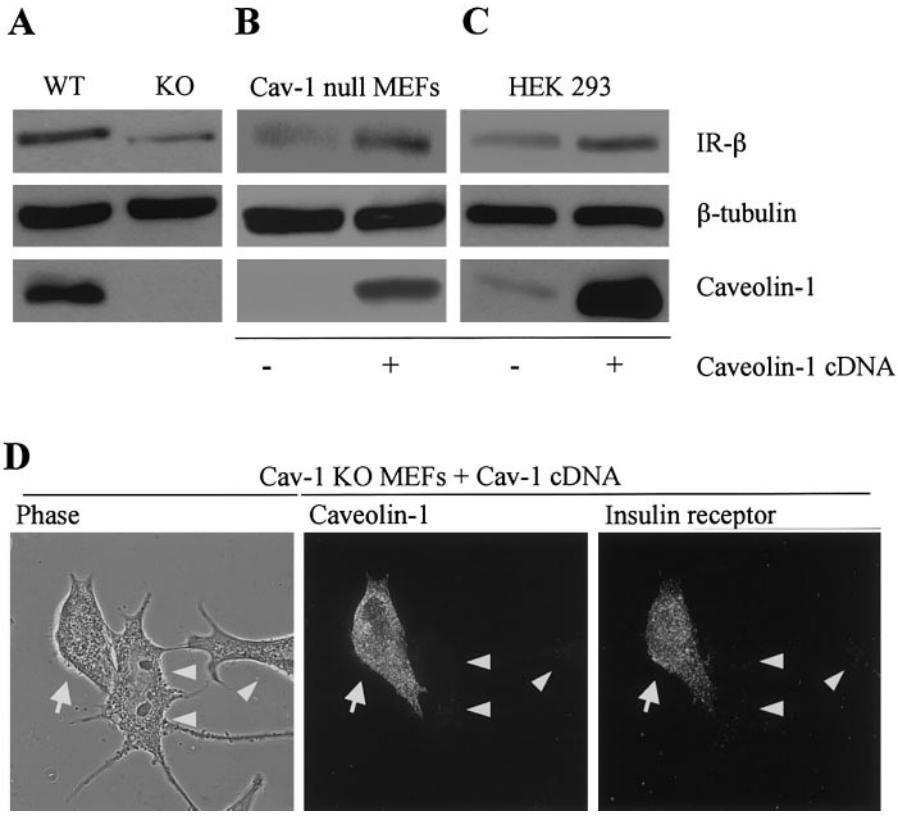

Fig. 10. Recombinant expression of caveolin-1 rescues IR-β expression, as assessed by Western blot and immunofluorescence microscopy. *A*: lysates from WT and Cav-1 KO mouse embryonic fibroblasts (MEFs) were analyzed by SDS-PAGE and Western blotting. Note that WT MEFs contain significantly more IR-β than Cav-1 KO MEFs. Thus this 3T3 fibroblast cell culture system demonstrates the same phenotype observed in adipose tissue derived from whole animals. *B*: Cav-1 null MEFs were transiently transfected with the full-length cDNA encoding caveolin-1 (+, pCB7-Cav-1) or vector alone (−, pCB7). Thirty-six hours posttransfection, cell lysates were prepared and subjected to immunoblot analysis with antibodies specific for IR-β. Note that recombinant expression of caveolin-1 dramatically rescued the expression of the IR-β. *C*: virtually identical results were obtained by transient transfection of HEK-293 cells with the caveolin-1 cDNA. These results show that recombinant expression of caveolin-1 in fibroblastic cells stabilizes IR-β expression. *D*: Cav-1 KO MEFs were transiently transfected with the full-length caveolin-1 cDNA, fixed, and doubly immunostained with antibodies directed against caveolin-1 (mouse MAb 2234; *middle*) and the IR-β (rabbit PAb; *right*). *Left*: phase contrast image; *middle*: caveolin-1 immunostaining; and *right*: insulin receptor (IR-β) immunostaining. Note that insulin receptor immunostaining was rescued in the caveolin-1-expressing cell (arrow); in contrast, neighboring untransfected cells (arrowheads) lack caveolin-1 expression and show little or no insulin receptor immunostaining.

DISCUSSION

In this study, we have clearly demonstrated an important new role for caveolin-1 in insulin signaling in the adipocyte. We have shown for the first time that postprandial hyperinsulinemia develops in Cav-1 null mice when they are fed a high-fat diet for 9 mo and that Cav-1 null mice on a normal chow diet demonstrate significant insulin resistance when challenged with an ITT. To explain these findings, we first examined tissues (other than adipose) for evidence of fatty depositions, as is often seen in the scenario of obesity leading to the development of type II diabetes in humans. However, the lipid content of skeletal muscle tissue derived from Cav-1 null mice remained unchanged compared with that of WT control mice. Thus we next examined the status of insulin receptor signaling in the adipocyte. By administering insulin via an intraperitoneal injection, we showed a significant decrease in

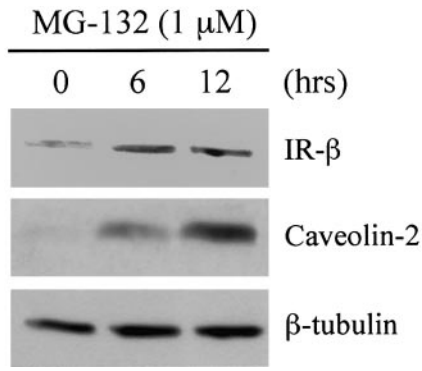

Fig. 11. Rescue of insulin receptor expression in Cav-1 null MEFs by the proteasomal inhibitor MG-132. Cav-1 null MEFs were treated with MG-132 (1 μM) for a series of time points (6 and 12 h) or with vehicle (Me_2SO) alone. Cell lysates were then analyzed by Western blot, which revealed an increase in IR-β protein content with MG-132 treatment. Caveolin-2 expression is shown as a positive control because it has previously been shown to be rescued by proteasomal inhibition (12). Equal protein loading was assessed with β-tubulin MAb.

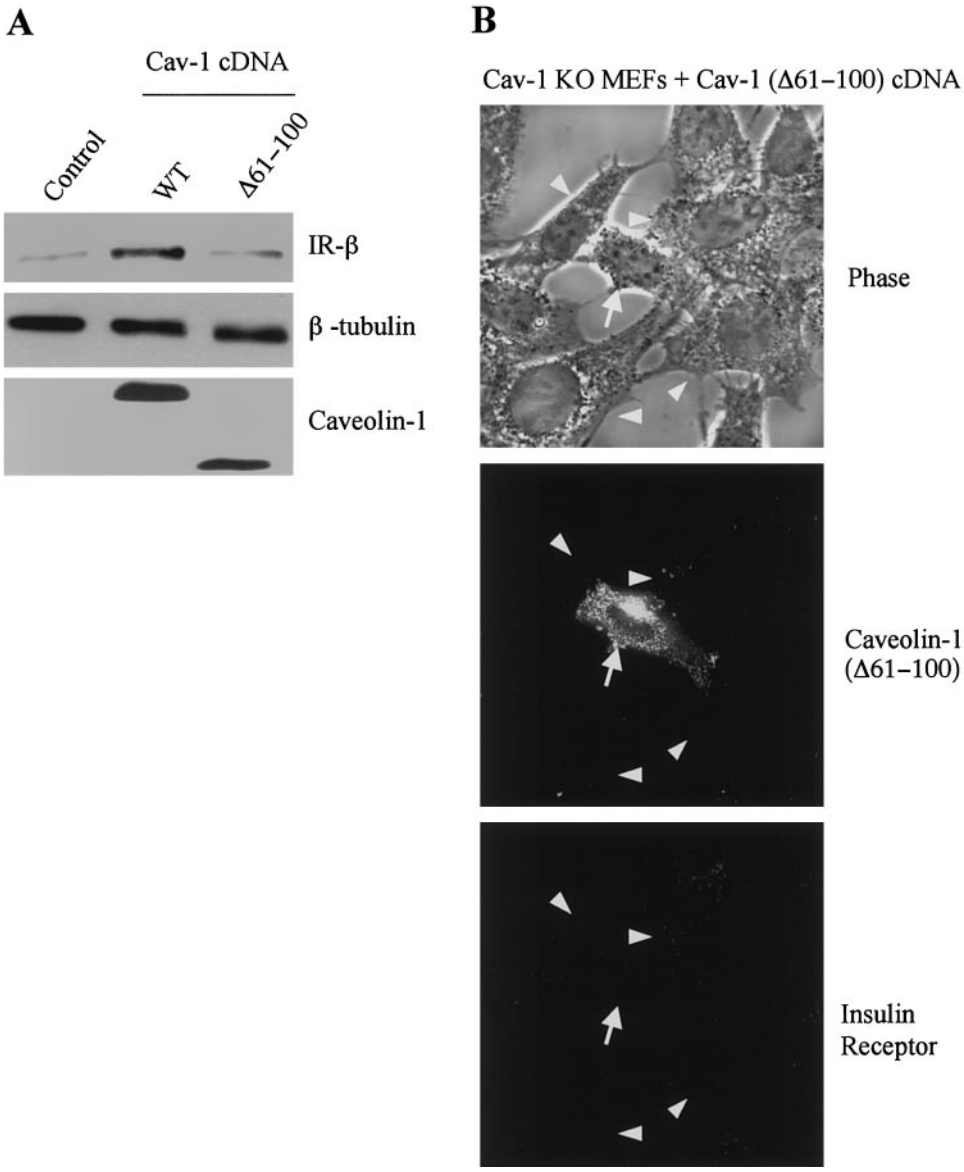

Fig. 12. Recombinant expression of Cav-1 (Δ61–100) fails to rescue IR-β protein expression. *A*: Cav-1 null MEFs were transiently transfected with cDNAs encoding either full-length WT Cav-1 (1–178) or an internal deletion mutant lacking the caveolin-scaffolding domain, Cav-1 (Δ61–100). Western blot analysis demonstrates that whereas transfection of the full-length WT Cav-1 cDNA was able to rescue IR-β protein levels, the mutant Cav-1 (Δ61–100) failed to rescue IR-β protein levels. *B*: Cav-1 KO MEFs were transiently transfected with the cDNA encoding Cav-1 (Δ61–100), fixed, and doubly immunostained with antibodies directed against caveolin-1 (mouse MAb 2234) and the IR-β (rabbit PAb). *Top*: phase-contrast image; *middle*: caveolin-1 immunostaining; and *bottom*: insulin receptor (IR-β) immunostaining. Note that there is no change in insulin receptor immunostaining in the caveolin-1 (Δ61–100)-expressing cell (arrow); similarly, neighboring untransfected cells (arrowheads) lack caveolin-1 expression and also show little or no insulin receptor immunostaining.

insulin-mediated phosphorylation of the IR-β subunit in Cav-1 null adipose tissue. Furthermore, we demonstrate that this blunted insulin receptor signaling is due to the dramatic downregulation of the IR-β subunit in Cav-1 null adipose tissue; IR-β subunit levels were reduced by >90% compared with WT controls. However, insulin receptor mRNA levels remained unchanged in Cav-1 null adipose tissue, suggesting the notion that caveolin-1 somehow stabilizes the insulin receptor at the protein level. Furthermore, in Cav-1 null mice, we showed that the insulin receptor protein is selectively downregulated only in the insulin-sensitive tissue that expresses an abundance of caveolin-1, i.e., adipose tissue. In striking contrast, other insulin-responsive tissues that normally express little or no caveolin-1, such as the liver and muscle, have normal levels of insulin receptor protein and exhibit the normal phosphorylation response to insulin stimulation. An analysis of the downstream targets of insulin action showed an increase in GLUT-4 and PKB/Akt levels, again only in the adipocyte, whereas other insulin-responsive proteins, GSK-3β, PI 3-kinase, and PP2A, remained undisturbed. Furthermore, we demonstrated that PKB/Akt and GSK-3β fail to respond to insulin administration in Cav-1 null mice, thus indicating that the decrease in insulin receptor levels does indeed have functional significance in Cav-1 null adipose tissue.

Next, by transient transfection of Cav-1 null 3T3 fibroblasts, we directly demonstrated that replacement of caveolin-1 is sufficient to rescue insulin receptor protein expression. Using the well-established inhibitor MG-132, we showed that in the absence of caveolin-1, the insulin receptor undergoes proteasomal degradation. Finally, we provided evidence that the caveolin-scaffolding domain is required to stabilize the insulin receptor, because the Cav-1 (Δ61–100) mutant failed to rescue insulin receptor expression in Cav-1 null MEFs. Using a cell-permeable peptide correspond-

Table 1. *Mutation of the caveolin-binding motif within the human insulin receptor is associated with insulin resistance and insulin receptor instability*

Insulin Receptor Caveolin-Binding Motif	Mutations and Associated Disease	References
1193 W S F G V V L W 1200	Wild type; normal	
L S F G V V L W	W1193L; severe insulin resistance	9, 10, 12, 35
W S F G V V L S	W1200S; severe insulin resistance	17,18

ing to the caveolin-1 scaffolding domain (15), we were able to demonstrate rescue of the insulin receptor in Cav-1 null MEFs, indicating that the scaffolding domain by itself is sufficient to functionally stabilize the insulin receptor (data not shown). Our results show that caveolin-1 is indeed an important positive regulator of insulin signaling, because it normally serves to stabilize the insulin receptor at the protein level in both fibroblasts and adipocytes. These studies are consistent with previous in vitro studies that demonstrated a direct interaction between caveolin-1 and the insulin receptor kinase domain (49).

Pathways of metabolic control are delicately balanced, and it is now clear that caveolin-1 plays an integral part in maintaining normal lipid homeostasis. Lipid balance is regulated by hormonal control in response to an ever changing environment. After a meal, insulin is released, having a multitude of effects on various tissues. In the adipocyte, regarding lipid compounds, insulin serves to activate the production of lipids in their storage form while inhibiting their breakdown. In Cav-1 null mice, it seems that this regulatory step is imbalanced or skewed toward overactive lipolysis. This is consistent with the idea that caveolin-1 functions to *1*) enhance insulin mediated lipogenic signals while *2*) suppressing the opposing PKA mediated lipolytic signals in the adipocyte (1, 13, 33, 34). This inhibition is due to both a direct negative effect of caveolin-1 on PKA and an indirect effect on PKA via augmentation of anti-lipolytic insulin signals (30). Insulin inhibits lipolysis by activating phosphodiesterase-3, which leads to a decrease in intracellular cAMP levels and a subsequent loss of activation of PKA (47). Insulin also causes a stable inhibitory complex to form between hormone sensitive lipase and lipotransin, the main lipolytic hormone in the adipocyte (43). In our study, we found that Cav-1-null mice have a blunted response to insulin and, presumably, an inability to inactivate PKA-mediated lipolysis.

The role that we have suggested for caveolin-1 in the regulation of insulin-dependent signals and the development of an insulin-resistant state is in line with the previously proposed role of caveolin-1 as an activator of insulin signaling in HEK-293 cells (49). In their report, Yamamoto et al. demonstrated that transient transfection of the cDNAs encoding full-length caveolin-1 or caveolin-3 proteins into HEK-293 cells was sufficient to increase IRS-1 phosphorylation following insulin stimulation. Furthermore, they demonstrated a direct interaction between the insulin receptor kinase domain and the caveolin-scaffolding domain of both caveolin-1 and caveolin-3. More specifically, the scaffolding domain of caveolin-1 (residues 82–101) binds to a specific motif in the kinase domain of the insulin receptor (^{1193}WSFGVVLW^{1200}; ΦXΦXXXXΦ, where Φ represents an aromatic amino acid) (4, 49). Thus they proposed that this caveolin-1/IR-β interaction somehow mediates the activation of the insulin receptor. Our new in vivo findings (described here) support this idea and show that the increased IRS-1 phosphorylation that Yamamoto et al. observed is most likely due to an increase in the insulin receptor protein itself, via a stabilizing interaction with caveolin-1. In further support of our findings, it has been shown that treatment with the lipid raft/caveolae-disrupting agent, methyl-β-cyclodextrin, inhibits insulin and insulin-like growth factor-1-induced activation of IRS-1 and the downstream activation of PKB/Akt (25, 26). Furthermore, these authors demonstrated that cells treated with methyl-β-cyclodextrin become insulin-resistant, in that they are no longer capable of glucose uptake. Our in vivo findings are consistent with these reports showing that insulin stimulation of Cav-1-deficient adipose tissue results in diminished activation of the insulin receptor and its downstream targets.

In another study, Nystrom et al. (21) systematically mutated the caveolin-binding motif within the insulin receptor kinase domain (W1193G/F1195G/W1200G). When transfected into COS-7 cells, they found that these caveolin-binding motif mutants were poorly expressed, compared with the WT insulin receptor (21). Together with our findings, this lack of insulin receptor expression demonstrates the critical need for a functional interaction between caveolin-1 and the insulin receptor to achieve normal receptor levels in certain cell types.

This idea can be further applied to the clinical setting. A subset of patients with severe insulin resistance has mutations within the caveolin-binding motif of the insulin receptor (W1193L and W1200S) (9, 10, 12, 17, 18, 35). These caveolin-binding motif mutations lead to enhanced degradation of the insulin receptor (12, 35) (Table 1). Thus a better understanding of the interaction between caveolin-1 and the insulin receptor may lead to the development of new therapies that functionally stabilize insulin receptor protein expression.

In this and our previous study demonstrating adipose tissue abnormalities (27), we found that Cav-1 null mice maintain relative euglycemia in the face of insulin resistance. To explain these findings, we examined the potential compensatory role of the IGF-1R. We found that there is no change in the amount of IGF-1R

protein levels in Cav-1 null adipose tissue, eliminating the IGF-1R as a major compensatory player. Therefore, a major impairment of insulin signaling at the level of the fat cell in Cav-1 null mice does not lead to the classic early manifestations of impaired glucose tolerance, i.e., normoglycemia associated with fasting hyperinsulinemia. Interestingly, in contrast to the generally decreased levels of GLUT-4 in obese and insulin-resistant models (40), we found an upregulation of the insulin-responsive glucose transporter, GLUT-4, that at least in part may explain the ability of Cav-1 null mice to sustain euglycemia despite local insulin resistance. Most importantly though, insulin receptor levels remain normal in the skeletal muscle tissue of Cav-1 null mice. Because ~75% of glucose is normally disposed of in skeletal muscle tissue, it is possible that the skeletal muscle compensates for adipose tissue in this regard (33). Also, in support of our findings, it is interesting to note that both the recently developed adipose-tissue selective insulin receptor knockout mouse (FIRKO) and the combined muscle and adipose tissue insulin receptor knockout mouse maintain euglycemia (2, 14).

Many recent studies have demonstrated that perhaps the most important determinant of insulin sensitivity is the lipid content of muscle and liver tissue. In the case of obesity or lipoatrophy, the adipocyte is unable to store lipids, and thus, triglycerides accumulate in muscle and liver. This leads to severe insulin resistance in these tissues and the eventual development of type II diabetes. Disease progression can be halted or even reversed in some cases when triglycerides, particularly in the muscle, are eliminated by oxidation. Recent evidence points to two adipokines, leptin and Acrp30, as being instrumental in this process. Leptin directly activates AMP-activated protein kinase in the muscle, which leads to fatty acid consumption, via oxidation, and the subsequent improvement of insulin sensitivity (8, 16, 41, 50). Similarly, Acrp30 has been reported to be involved in activating expression of molecules responsible for fatty acid transport and combustion in skeletal muscle (50). Thus it seems that the adipocyte is the primary player in the progression of insulin resistance, with the muscle and liver being the determinants of how far the disease will progress. Given that liver and skeletal muscle express normal levels of insulin receptor in Cav-1 null mice, this could explain why we observed euglycemia and a relatively mild postprandial hyperinsulinemia in Cav-1 null animals.

Recently, using the Cre-loxP system, Blüher and colleagues (2) developed a FIRKO mouse. Because this mouse lacks the insulin receptor specifically in adipocytes, as does the Cav-1 null mouse, a discussion of this model is highly relevant. Important similarities between these two mouse models include resistance to age-related obesity, diminished body fat, and normal fasted and fed glucose levels on a chow diet, as well as normal fed insulin levels on a chow diet. However, these two mice differ substantially on many other parameters. Most related to the work reported here, FIRKO mice respond normally to an ITT even at 10 mo, an age when WT mice show significant insulin resistance. The authors claim (2) that this represents protection against obesity-related insulin intolerance, because their mice are lean at this age. However, Cav-1 null mice display a markedly blunted response to insulin at 5 mo of age, even though Cav-1 null mice are also resistant to age-related obesity. Other pertinent differences between these two mouse models include decreased brown fat mass in FIRKO mice (which is dramatically increased in Cav-1 null mice), increased plasma leptin and Acrp30 levels in FIRKO mice (which are decreased in Cav-1 null mice), and reduced serum triglyceride levels in FIRKO mice (which are markedly elevated in Cav-1 null mice). Several possibilities exist to explain these differences. Most importantly, the loss of caveolin-1 may have pleiotropic effects on multiple organ systems, signaling cascades, and cellular functions, the extent of which are just now being explored. Hosts of signaling molecules are known to localize to and signal through caveolae, only one of which is the insulin receptor. Therefore, it would be expected that dysregulation of many of these different cascades would lead to multiple independent, yet overlapping phenotypes. Yet, our results clearly demonstrate that caveolin-1 plays a significant role in insulin signal transduction via stabilization of the receptor.

The degree of insulin resistance found in Cav-1 null mice does not result in fasting hyperinsulinemia. This is in contrast to conventional models of type II diabetes. Similar findings have recently been observed in the FIRKO mouse. The FIRKO mice show no fasting hyperinsulinemia despite significant tissue-specific insulin resistance, as evidenced by impaired insulin-dependent glucose uptake in isolated adipocytes (2). However, the FIRKO mouse does not display whole body fasting or postprandial hyperinsulinemia. In fact, it maintains normal or below average insulin levels throughout its life. Thus the FIRKO mouse model indicates that insulin resistance in adipose tissue per se does not lead to fasting hyperinsulinemia. In light of this, the finding that Cav-1 null mice only display postprandial hyperinsulinemia is very much in line with the observations made in the FIRKO mouse model.

It is important to note that Cav-1 null mice are functionally deficient in caveolin-2 as well. Caveolin-1 and -2 form a functional heterooligomeric complex in cells where they are coexpressed (36). Caveolin-2 requires coexpression with caveolin-1; in the absence of caveolin-1, caveolin-2 remains trapped in the Golgi complex and undergoes proteasomal degradation (24). Therefore, all of the phenotypes identified in the Cav-1-null mouse must also be examined in the Cav-2-null mouse to determine whether the findings are due to a functional caveolin-2 deficiency. Importantly, we have recently shown that Cav-2-null mice do not show any lipid imbalances or adipose tissue atrophy, indicating that the adipose tissue abnormalities observed in Cav-1-null mice are indeed due to the loss of caveolin-1 expression and are not caveolin-2 dependent. Consis-

tent with these findings, we showed here that Cav-2-null mice express normal levels of IR-β in their adipose tissue. Thus caveolin-2 expression is not required for maintaining normal insulin receptor expression levels in the adipocyte.

We thank Dr. Roberto Campos-Gonzalez (BD Transduction Laboratories) for generously donating antibodies directed against caveolin-1, -2, and -3.

This work was supported by grants from the National Institutes of Health (NIH), Muscular Dystrophy Association, American Heart Association, and Breast Cancer Alliance (all to M. P. Lisanti) and by National Institute of Diabetes and Digestive and Kidney Diseases Grant R01-DK-55758 and a grant from the American Diabetes Association (to P. E. Scherer). A. W. Cohen, B. Razani, and T. M. Williams were supported by NIH Medical Scientist Training Grant T32-GM-07288. M. P. Lisanti is the recipient of a Hirschl/Weil-Caulier Career Scientist Award. T. P. Combs was supported by NIH Hormones/Membrane Interactions Training Grant T32-DK-07513-15.

REFERENCES

1. **Bickel PE.** Lipid rafts and insulin signaling. *Am J Physiol Endocrinol Metab* 282: E1–E10, 2002.
2. **Blüher M, Michael MD, Peroni OD, Ueki K, Carter N, Kahn BB, and Kahn CR.** Adipose tissue selective insulin receptor knockout protects against obesity and obesity-related glucose intolerance. *Dev Cell* 3: 25–38, 2002.
3. **Charron MJ, Katz EB, and Olson AL.** GLUT4 gene regulation and manipulation. *J Biol Chem* 274: 3253–3256, 1999.
4. **Couet J, Sargiacomo M, and Lisanti MP.** Interaction of a receptor tyrosine kinase, EGF-R, with caveolins. Caveolin binding negatively regulates tyrosine and serine/threonine kinase activities. *J Biol Chem* 272: 30429–30438, 1997.
5. **Cusin I, Terrettaz J, Rohner-Jeanrenaud F, Zarjevski N, Assimacopoulos-Jeannet F, and Jeanrenaud B.** Hyperinsulinemia increases the amount of GLUT4 mRNA in white adipose tissue and decreases that of muscles: a clue for increased fat depot and insulin resistance. *Endocrinology* 127: 3246–3248, 1990.
6. **Drab M, Verkade P, Elger M, Kasper M, Lohn M, Lauterbach B, Menne J, Lindschau C, Mende F, Luft FC, Schedl A, Haller H, and Kurzchalia TV.** Loss of caveolae, vascular dysfunction, and pulmonary defects in caveolin-1 gene-disrupted mice. *Science* 293: 2449–2452, 2001.
7. **Eldar-Finkelman H, Schreyer SA, Shinohara MM, LeBoeuf RC, and Krebs EG.** Increased glycogen synthase kinase-3 activity in diabetes- and obesity-prone C57BL/6J mice. *Diabetes* 48: 1662–1666, 1999.
8. **Friedman J.** Fat in all the wrong places. *Nature* 415: 268–269, 2002.
9. **Imamura T, Haruta T, Takata Y, Usui I, Iwata M, Ishihara H, Ishiki M, Ishibashi O, Ueno E, Sasaoka T, and Kobayashi M.** Involvement of heat shock protein 90 in the degradation of mutant insulin receptors by the proteasome. *J Biol Chem* 273: 11183–11188, 1998.
10. **Imamura T, Takata Y, Sasaoka T, Takada Y, Morioka H, Haruta T, Sawa T, Iwanishi M, Hu YG, Suzuki Y, Hamada J, and Kobayashi M.** Two naturally occurring mutations in the kinase domain of insulin receptor accelerate degradation of the insulin receptor and impair the kinase activity. *J Biol Chem* 269: 31019–31027, 1994.
11. **Iverson SJ, Lang SL, and Cooper MH.** Comparison of the Bligh and Dyer and Folch methods for total lipid determination in a broad range of marine tissue. *Lipids* 36: 1283–1287, 2001.
12. **Iwanishi M, Haruta T, Takata Y, Ishibashi O, Sasaoka T, Egawa K, Imamura T, Naitou K, Itazu T, and Kobayashi M.** A mutation (Trp1193→Leu1193) in the tyrosine kinase domain of the insulin receptor associated with type A syndrome of insulin resistance. *Diabetologia* 36: 414–422, 1993.
13. **Kersten S.** Mechanisms of nutritional and hormonal regulation of lipogenesis. *EMBO Rep* 2: 282–286, 2001.
14. **Lauro D, Kido Y, Castle AL, Zarnowski MJ, Hayashi H, Ebina Y, and Accili D.** Impaired glucose tolerance in mice with a targeted impairment of insulin action in muscle and adipose tissue. *Nat Genet* 20: 294–298, 1998.
15. **Liu J, Wang XB, Park DS, and Lisanti MP.** Caveolin-1 expression enhances endothelial capillary tubule formation. *J Biol Chem* 277: 10661–10668, 2002.
16. **Minokoshi Y, Kim YB, Peroni OD, Fryer LG, Muller C, Carling D, and Kahn BB.** Leptin stimulates fatty-acid oxidation by activating AMP-activated protein kinase. *Nature* 415: 339–343, 2002.
17. **Moller DE, Benecke H, and Flier JS.** Biologic activities of naturally occurring human insulin receptor mutations. Evidence that metabolic effects of insulin can be mediated by a kinase-deficient insulin receptor mutant. *J Biol Chem* 266: 10995–11001, 1991.
18. **Moller DE, Yokota A, Ginsberg-Fellner F, and Flier JS.** Functional properties of a naturally occurring Trp1200-Ser1200 mutation of the insulin receptor. *Mol Endocrinol* 4: 1183–1191, 1990.
19. **Mora A, Sabio G, Risco AM, Cuenda A, Alonso JC, Soler G, and Centeno F.** Lithium blocks the PKB and GSK3 dephosphorylation induced by ceramide through protein phosphatase-2A. *Cell Signal* 14: 557–562, 2002.
20. **Nakae J, Kido Y, and Accili D.** Distinct and overlapping functions of insulin and IGF-I receptors. *Endocr Rev* 22: 818–835, 2001.
21. **Nystrom FH, Chen H, Cong LN, Li Y, and Quon MJ.** Caveolin-1 interacts with the insulin receptor and can differentially modulate insulin signaling in transfected Cos-7 cells and rat adipose cells. *Mol Endocrinol* 13: 2013–2024, 1999.
22. **Okamoto T, Schlegel A, Scherer PE, and Lisanti MP.** Caveolins, a family of scaffolding proteins for organizing "pre-assembled signaling complexes" at the plasma membrane. *J Biol Chem* 273: 5419–5422, 1998.
23. **Palade GE.** Fine structure of blood capillaries (Abstract). *J Appl Physiol* 24: 1424, 1953.
24. **Parolini I, Sargiacomo M, Galbiati F, Rizzo G, Grignani F, Engelman JA, Okamoto T, Ikezu T, Scherer PE, Mora R, Rodriguez-Boulan E, Peschle C, and Lisanti MP.** Expression of caveolin-1 is required for the transport of caveolin-2 to the plasma membrane. Retention of caveolin-2 at the level of the Golgi complex. *J Biol Chem* 274: 25718–25725, 1999.
25. **Parpal S, Karlsson M, Thorn H, and Stralfors P.** Cholesterol depletion disrupts caveolae and insulin receptor signaling for metabolic control via insulin receptor substrate-1, but not for mitogen-activated protein kinase control. *J Biol Chem* 276: 9670–9678, 2001.
26. **Podar K, Tai YT, Cole CE, Hideshima T, Sattler M, Hamblin A, Mitsiades N, Schlossman RL, Davies FE, Morgan GJ, Munshi NC, Chauhan D, and Anderson KC.** Essential role of caveolae in interleukin-6- and insulin-like growth factor I-triggered Akt-1-mediated survival of multiple myeloma cells. *J Biol Chem* 278: 5794–5801, 2003.
27. **Razani B, Combs TP, Wang XB, Frank PG, Park DS, Russell RG, Li M, Tang B, Jelicks LA, Scherer PE, and Lisanti MP.** Caveolin-1 deficient mice are lean, resistant to diet-induced obesity, and show hyper-triglyceridemia with adipocyte abnormalities. *J Biol Chem* 277: 8635–8647, 2001.
28. **Razani B, Engelman JA, Wang XB, Schubert W, Zhang XL, Marks CB, Macaluso F, Russell RG, Li M, Pestell RG, Di Vizio D, Hou H Jr, Kneitz B, Lagaud G, Christ GJ, Edelmann W, and Lisanti MP.** Caveolin-1 null mice are viable but show evidence of hyperproliferative and vascular abnormalities. *J Biol Chem* 276: 38121–38138, 2001.
29. **Razani B and Lisanti MP.** Caveolin-deficient mice: insights into caveolar function and human disease. *J Clin Invest* 108: 1553–1561, 2001.
30. **Razani B, Rubin CS, and Lisanti MP.** Regulation of cAMP-mediated signal transduction via interaction of caveolins with the catalytic subunit of protein kinase A. *J Biol Chem* 274: 26353–26360, 1999.
31. **Razani B, Wang XB, Engelman JA, Battista M, Lagaud G, Zhang XL, Kneitz B, Hou H Jr, Christ GJ, Edelmann W,**

and Lisanti MP. Caveolin-2-deficient mice show evidence of severe pulmonary dysfunction without disruption of caveolae. *Mol Cell Biol* 22: 2329–2344, 2002.
32. **Rothberg KG, Heuser JE, Donzell WC, Ying Y, Glenney JR, and Anderson RGW.** Caveolin, a protein component of caveolae membrane coats. *Cell* 68: 673–682, 1992.
33. **Saltiel AR and Kahn CR.** Insulin signalling and the regulation of glucose and lipid metabolism. *Nature* 414: 799–806, 2001.
34. **Saltiel AR and Pessin JE.** Insulin signaling pathways in time and space. *Trends Cell Biol* 12: 65–71, 2002.
35. **Sawa T, Imamura T, Haruta T, Sasaoka T, Ishiki M, Takata Y, Takada Y, Morioka H, Ishihara H, Usui I, and Kobayashi M.** Hsp70 family molecular chaperones and mutant insulin receptor: differential binding specificities of BiP and Hsp70/Hsc70 determines accumulation or degradation of insulin receptor. *Biochem Biophys Res Commun* 218: 449–453, 1996.
36. **Scherer PE, Lewis RY, Volonte D, Engelman JA, Galbiati F, Couet J, Kohtz DS, van Donselaar E, Peters P, and Lisanti MP.** Cell-type and tissue-specific expression of caveolin-2. Caveolins 1 and 2 co-localize and form a stable heterooligomeric complex in vivo. *J Biol Chem* 272: 29337–29346, 1997.
37. **Scherer PE, Okamoto T, Chun M, Nishimoto I, Lodish HF, and Lisanti MP.** Identification, sequence and expression of caveolin-2 defines a caveolin gene family. *Proc Natl Acad Sci USA* 93: 131–135, 1996.
38. **Scherer PE, Tang ZL, Chun MC, Sargiacomo M, Lodish HF, and Lisanti MP.** Caveolin isoforms differ in their N-terminal protein sequence and subcellular distribution: identification and epitope mapping of an isoform-specific monoclonal antibody probe. *J Biol Chem* 270: 16395–16401, 1995.
39. **Shigematsu S, Watson RT, Khan AH, and Pessin JE.** The adipocyte plasma membrane caveolin functional/structural organization is necessary for the efficient endocytosis of GLUT4. *J Biol Chem* 278: 10683–10690, 2002.
40. **Shimaya A, Noshiro O, Hirayama R, Yoneta T, Niigata K, and Shikama H.** Insulin sensitizer YM268 ameliorates insulin resistance by normalizing the decreased content of GLUT4 in adipose tissue of obese Zucker rats. *Eur J Endocrinol* 137: 693–700, 1997.
41. **Shimomura I, Hammer RE, Ikemoto S, Brown MS, and Goldstein JL.** Leptin reverses insulin resistance and diabetes mellitus in mice with congenital lipodystrophy. *Nature* 401: 73–76, 1999.
42. **Sotgia F, Razani B, Bonuccelli G, Schubert W, Battista M, Lee H, Capozza F, Schubert AL, Minetti C, Buckley JT, and Lisanti MP.** Intracellular retention of GPI-linked proteins in caveolin-deficient cells. *Mol Cell Biol* 22: 3905–3926, 2002.
43. **Syu LJ and Saltiel AR.** Lipotransin: a novel docking protein for hormone-sensitive lipase. *Mol Cell* 4: 109–115, 1999.
44. **Tang ZL, Scherer PE, Okamoto T, Song K, Chu C, Kohtz DS, Nishimoto I, Lodish HF, and Lisanti MP.** Molecular cloning of caveolin-3, a novel member of the caveolin gene family expressed predominantly in muscle. *J Biol Chem* 271: 2255–2261, 1996.
45. **Toya Y, Yamamoto M, Schwencke C, Lisanti MP, Myers M, and Ishikawa Y.** Caveolin is an activator of insulin receptor signaling. *J Biol Chem* 273: 26962–26968., 1998.
46. **Watson RT and Pessin JE.** Subcellular compartmentalization and trafficking of the insulin-responsive glucose transporter, GLUT4. *Exp Cell Res* 271: 75–83, 2001.
47. **Wijkander J, Landstrom TR, Manganiello V, Belfrage P, and Degerman E.** Insulin-induced phosphorylation and activation of phosphodiesterase 3B in rat adipocytes: possible role for protein kinase B but not mitogen-activated protein kinase or p70 S6 kinase. *Endocrinology* 139: 219–227, 1998.
48. **Yamada E.** The fine structure of the gall bladder epithelium of the mouse. *J Biophys Biochem Cytol* 1: 445–458, 1955.
49. **Yamamoto M, Toya Y, Schwencke C, Lisanti MP, Myers M, and Ishikawa Y.** Caveolin is an activator of insulin receptor signaling. *J Biol Chem* 273: 26962–26968, 1998.
50. **Yamauchi T, Kamon J, Waki H, Terauchi Y, Kubota N, Hara K, Mori Y, Ide T, Murakami K, Tsuboyama-Kasaoka N, Ezaki O, Akanuma Y, Gavrilova O, Vinson C, Reitman ML, Kagechika H, Shudo K, Yoda M, Nakano Y, Tobe K, Nagai R, Kimura S, Tomita M, Froguel P, and Kadowaki T.** The fat-derived hormone adiponectin reverses insulin resistance associated with both lipoatrophy and obesity. *Nat Med* 7: 941–946, 2001.